Highlights

Optimizing magnetometers arrays and pre-processing pipelines for multivariate pattern analysis

Yulia Bezsudnova, Ole Jensen

- Using signal space separation on magnetometer data prior to multivariate pattern analysis might reduce classification accuracy as it reduces the rank of the data resulting in loss of information.
- When performing multivariate data analysis, other noise reduction approaches that reduce the rank of the data less are advisable such as signal space projection or 3rd-order gradient noise reduction.
- A sensor array of about 25 magnetometers is sufficient for multivariate pattern analysis.

Optimizing magnetometers arrays and pre-processing pipelines for multivariate pattern analysis

Yulia Bezsudnova[a], Ole Jensen[b]

[a] *Centre for Human Brain Health, School of Physics and Astronomy, University of Birmingham, Edgbaston, Birmingham, B15 2TT, , United Kingdom*
[b] *Centre for Human Brain Health, School of Psychology, University of Birmingham, Edgbaston, Birmingham, B15 2TT, , United Kingdom*

Abstract

Multivariate pattern analysis (MVPA) has proven an excellent tool in cognitive neuroscience for identifying representational-specific neuronal patterns using EEG, MEG, and MRI. Likewise, it also holds a strong promise when applied to optically-pumped magnetometer-based magnetoencephalography (OPM-MEG) data. To optimize OPM-MEG systems for MVPA experiments this study examines data from conventional MEG magnetometer arrays, focusing on appropriate noise reduction techniques for magnetometers and determining the optimal number of sensors for effective MVPA. We found that the use of signal space separation (SSS) aimed at projecting out the noise contributions not generated by the brain, significantly lowered the classification accuracy considering the 102 magnetometers. Therefore, we advise against SSS filters for magnetometers when performing MVPA. Instead, we recommend employing noise reduction techniques like signal-space projection, independent component analysis (ICA), or third-order gradient noise reduction based on reference sensors to enhance MVPA performance. We also tested how many magnetometers were required for multivariate pattern analysis. We found that classification accuracy did not improve when going beyond 25 sensors. In conclusion, when designing an MEG system based on SQUID or OPM magnetometers which is optimized for multivariate analysis, about 25 magnetometers are sufficient possibly augmented with reference sensors for noise reduction.

Keywords: Signal Space Separation filter, Maxwel Filter, MVPA, Magnetoencephalography, Magnetometers, Optimization, Optically pumped magnetometers,

1. Introduction

Multivariate pattern analysis (MVPA) is an established methodology for functional MRI, MEG, and EEG. MVPA operates by classifying the spatial distribution of brain activity associated with representing different objects' classes or experimental conditions (Haxby et al., 2001; Haynes and Rees, 2006; Pereira et al., 2009; Grootswagers et al., 2017; Carlson et al., 2019; Stokes et al., 2015; Cichy et al., 2014). If spatial patterns of brain activation successfully predict condition or stimulus category, it implies the presence of relevant information related to the experimental manipulation within the neuroimaging data. This property facilitates a crucial connection between theory and data. Furthermore, applying MVPA in the context of representational similarity analysis (RSA) allows to fuse the data from BOLD measures obtained from fMRI and electrophysiological data obtained from EEG/MEG, leading to an enhanced understanding of the brain's spatio-temporal properties in relation to neuronal responses (Kriegeskorte and Kievit, 2013; Guggenmos et al., 2018; Kriegeskorte et al., 2008; Kriegeskorte, 2009; Diedrichsen and Kriegeskorte, 2017). Overall, MVPA applied for classification approaches and RSA is a powerful tool for cognitive neuroscience widely used to study object recognition (Cichy et al., 2014; Proklova et al., 2016; Cichy et al., 2016; Kaplan et al., 2015; Dirani and Pylkkänen, 2023) or other cognitive brain functions like prediction, spatial navigation, memory and emotions (Frisby et al., 2023; Harrison and Tong, 2009; Kornysheva et al., 2019; Brown et al., 2016; Ariani et al., 2022; King and Dehaene, 2014; Wang et al., 2018).

This study lays the groundwork for exploring the potential benefits of utilizing on-scalp optically pumped magnetometer based magnetoencephalography (OPM-MEG) in experiments designed for MVPA. There are two main reasons why MVPA stands to benefit from OPM-MEG systems. First, OPMs can be put directly on the subject head and therefore the magnitude of the MEG signal is stronger compared to the signal obtained by SQUID-MEG systems (Brookes et al., 2022; Bezsudnova et al., 2022). Second, the sensors can be arranged in an array that better captures the spatial characteristics of the brain signal (Beltrachini et al., 2021; Iivanainen et al., 2017; Brookes et al., 2021). As a result, OPM-MEG potentially has higher sensitivity and better spatial resolution than conventional MEG systems, which is beneficial for MVPA (Labyt et al., 2022). While OPM-MEG is still in its early stages

of development and specific engineering challenges have to be solved, a study conducted by (Nugent et al., 2022) demonstrates the theoretical capability of a dense OPM array to effectively resolve multiple independent electrophysiological sources to a degree currently achievable only using an invasive technique.

Notably, conventional MEG studies typically involve the analysis of gradiometers due to their lower sensitivity to external noise sources (Vrba and Robinson, 2001); however, current OPM-MEG systems utilize only magnetometers (Rea et al., 2022). Therefore, to pave the way for optimizing MVPA used with OPM-MEG, this study focuses on data obtained from a conventional MEG magnetometer array. Specifically, we explore appropriate noise reduction techniques for magnetometers and investigate the optimal number of sensors required to achieve adequate MVPA performance.

2. Methods

2.1. Experimental paradigm

In this study, we investigated the time course of the emergence of semantic representations using picture stimuli employing MVPA applied to conventional SQUID MEG data.

Thirty-eight healthy native English adult participants took part in the study. Five participants were excluded due to excessive noise in the data, two participants were excluded due to poor performance (¿15% wrong answer), therefore the final data set consists of recordings from thirty-one participants (mean age ± SD = 21.77 ± 3.31; 21 females). The study was conducted at the Centre for Human Brain Health. The University of Birmingham Ethics Committee approved the study. Participants were compensated with credits or a monetary reward.

The stimulus set was composed of 48 objects. The objects were organized as in (Iamshchinina et al., 2022) according to three types of categories, each divided into two groups: size (big/small), movement (moving/still), and nature (natural/man-made). Each object in the study was part of one of the sub-categories(Fig. 1 e.g. a book is small, still, and man-made). The stimulus set was balanced such that each categorical division included one-half of the stimulus set (24 objects). Hence each set of sub-categories (e.g. big, still, natural) included 6 objects. The selection of category divisions in this study was based on previous findings demonstrating reliable neural representations of semantic dimensions across categories (Huth et al., 2012; Konkle

and Caramazza, 2013). For other purposes not to be analysed here, each object is presented in two modalities: written words and pictures. The size of the images was 400 x 400 pixels. Prior to the object presentation, the fixation cross was shown for 0.5-0.7 s. Each object was presented for 0.6 s. The experiment was divided into 9 blocks where either the succession of words (5 blocks) or images (4 blocks) was presented. After each block, a participant had a break. Each stimulus was present 4 times in a block. We used a two-alternative forced choice task (question trial) that used stimuli from the other modality than the current block. As such a participant had to identify the correct picture during the written words and vice versa. The study was designed to engage participants and encourage deep processing of stimuli in a cross-modal manner. Note that in each block the question trial was applied for every unique object once and alternative choices were unique as well. The design is shown in Figure 1.

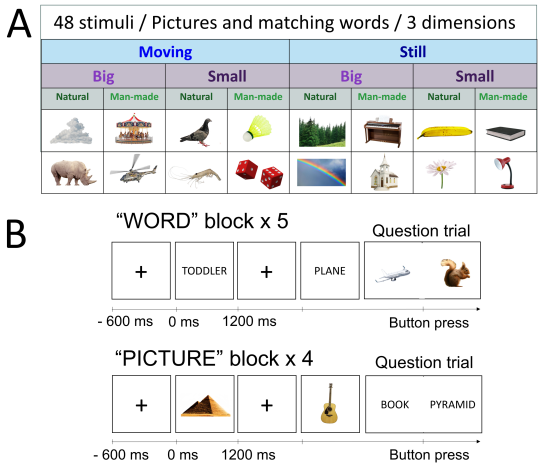

Figure 1: Experimental paradigm. A) The stimulus set is comprised of 48 objects which can be divided according to 3 dimensions ("size": big/small; "movement": still/moving; "nature": natural/man-made). B) In both image and word blocks, participants were presented with stimuli in random order. In the picture block, participants viewed images of the objects, while in the word block, they read the corresponding words. The task (question trial) was presented randomly every fifth trial on average. Participants were required to identify whether the picture or word corresponded to a previously seen stimulus and press the appropriate button accordingly. When pictures were presented the probe question was presented as a word and vice versa.

In each block, a randomly selected stimulus was presented on a grey screen

at a visual angle of 6°. The stimuli presentation is implemented in Matlab using the Psychophysics Toolbox Brainard and Vision (1997).

2.2. MEG recording

MEG data were recorded using a 306-sensor TRIUX Elekta Neuromag system, consisting of 204 orthogonal planar gradiometers and 102 magnetometers, with online band-pass filtering from 0.1 to 330 Hz and a sampling rate of 1000 Hz. Prior to data acquisition, the locations of three bony fiducial points (nasion, left and right preauricular points) were digitized using a Polhemus Fastrack electromagnetic digitizer system. Additionally, four head-position indicator coils (HPI coils) were digitized: two on the left and right mastoid bone and two on the forehead, spaced at least 3 cm apart. To facilitate the spatial co-registration of MEG source analysis with individual structural MRI images, a minimum of 400 extra scalp points were acquired for each participant. Following these preparations, participants were positioned upright with a 60° angle backrest under the MEG gantry. To record the horizontal EOG, a pair of electrodes was attached approximately 2.5 cm away from the outer canthus of each eye. To record the vertical EOG, a pair of electrodes was placed above and below the right eye in line with the pupil. The ECG was recorded from a pair of electrodes placed on the left and right collarbone.

2.3. Standard data processing pipeline

Only data from viewing picture blocks was used in this study. The data was analysed using the open-source toolbox MNE Python v0.24.0 (Gramfort et al., 2013) following the standards defined in the FLUX Pipeline (Ferrante et al., 2022). The standard MVPA pipeline for a conventional MEG consists of the following steps.

First, blinks and muscle artefacts were annotated using EOG channels and magnetometers' recordings respectively. A semi-automatic detection algorithm was utilized to mark sensors with excessive artefacts (on average 4.5 sensors per participant). Then, the data was low-pass filtered at 100 Hz to reduce HPI coils artefacts.

As a next step, conventionally, Signal-Space Separation (SSS) and Maxwell filtering are applied to reduce magnetic artefacts from the environment. The SSS method is a spatial method that transforms electromagnetic multichannel data into uncorrelated basic components, e.g. magnetic multipole moments and reconstructs the data using only those moments originating in-

side the brain. The origin, e.g. brain-related or external interference signals, of these magnetic field components is defined based on sensor geometry and Maxwell's equations only. All external origin components are dropped such that the signal is reconstructed mainly from the brain-related components (Taulu and Kajola, 2005). Maxwell filtering is a related procedure that removes the higher-order components of the internal subspace, which are mainly dominated by sensor noise. Typically, Maxwell filtering and SSS are performed together (in MNE-Python they are implemented together in a single function) (Gramfort et al., 2013; Taulu and Simola, 2006). From here on, we will refer to this step using the term "SSS filtering" or SSS. While SSS significantly reduces noise from interfering sources, it results in a substantial rank reduction of the data, typically from hundreds of dimensions to a significantly lower number (from about 306 to 65 dimensions for a typical MEGIN system) (Taulu and Kajola, 2005).

As mentioned in the introduction, this study is focused on finding appropriate noise-reduction techniques for magnetometers. The alternative method to SSS filtering to reduce environmental noise is the signal-space projection (SSP) technique (Uusitalo and Ilmoniemi, 1997). SSP relies on the fact that the magnetic field distributions generated by the sources in the brain have spatial distributions sufficiently different from those generated by external noise sources. SSP operates by detecting characteristic sensor topographies related to specific artefacts, typically based on a prior principle component analysis of empty room recordings, and subsequently generating spatial projectors to effectively eliminate the influence of these artefact-related topographies from the data (Haumann et al., 2016). This procedure typically reduces the rank of the data by about 8 components.

In this work, we excluded Independent Component Analysis step, which is typically used to remove components associated with cardiac artefacts and eyeblinks (Hyvärinen and Oja, 2000)), to examine how various filtering methods affect classification accuracy. Next, data is segmented into trials. Trials corresponding to the same stimulus are averaged together to construct "supertrials". This step again increases the signal-to-noise of the data (Ashton et al., 2022; Guggenmos et al., 2018).

In this study, we downsampled the data to 500 Hz. Epochs are cropped to 100 ms before stimuli onset and 700 ms after. Each time point was represented as a 306-dimensional vector (channel data). We expanded this vector by adding past 25 ms (12 time points) and future 25 ms (12 time points) of data, resulting in 306x25 dimensional feature vector representing each time

point. This procedure (termed "delayed embedding") resulted in a more information-rich representation of the neural activity associated with a given stimulus by incorporating more time points (Chan et al., 2011; Tyler et al., 2013; Cheng, 2021). This feature vector was then used in the classifier.

Multivariate pattern analysis was applied to the pre-processed MEG data to classify the categories of the presented objects. Prior to classification, the data was standardized by removing the mean and scaling to unit variance per sensor. Subsequently, we employed a support vector machine (SVM) (Cortes and Vapnik, 1995) from the Python module Scikit-learn (Pedregosa et al., 2011) to classify the data over time. The classification procedure relied on a 5-fold cross-validation approach, and the performance was quantified using the area under the curve (AUC) metric, which measures the classifier discriminative ability.

2.4. Number of channels

We also asked how many magnetometers are needed to get good classification accuracy results. We also asked how many magnetometers are needed to get good classification accuracy results. We randomly selected N magnetometers, spaced equidistantly, from the existing pool of 102 sensors. N was varied from 7 to 102 with step 5. The data from the chosen set of sensors were organized into a feature vector, which included 25 ms of past and future time points. This feature vector was subsequently fed into the classifier.

3. Results

We aimed to examine appropriate noise reduction methods for magnetometers and determine the optimal number of sensors required to achieve adequate MVPA performance. This investigation sets the groundwork and speaks to design considerations for future studies utilizing MVPA applied to OPM-MEG systems.

The study is based on conventional SQUID-MEG data recorded when participants were looking at pictures of objects from different categories: size (big/small), movement (still/moving), nature (natural/man-made; see Fig. 1). We compared the MVPA classification accuracy curves for different pre-processing pipelines. The pipeline labelled as "SSP" employed the SSP algorithm for noise reduction without the use of any bad channel rejection. The "SSS filter" pipeline used the SSS filter as it is implemented in the MNE

Python package (Gramfort et al., 2013). The pipeline labelled as "raw" did not involve any noise reduction algorithms.

Unlike gradiometers, which attenuate noise from distant sources by measuring the spatial gradient, magnetometers measure the absolute magnetic field and thus are highly susceptible to environmental noise. Consequently, the application of SSS filter or SSP filter that reduces external artefacts in the data substantially impacts magnetometer recordings. Fig. 2 shows the power spectra of magnetometer data before and after applying SSS and SSP filters, demonstrating a notable reduction of environmental noise particularly in the magnetometers recordings.

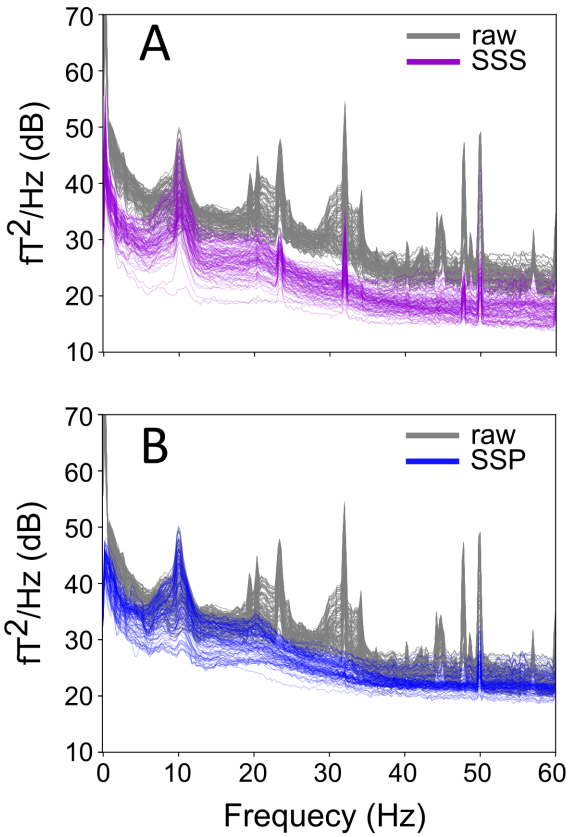

Figure 2: Power spectra of the magnetometer data. The grey lines represent the spectra prior to the application of noise reduction algorithms. A) The magenta lines depict data after the application of "SSS". B) The blue lines depict data after application of "SSP".

3.1. MaxFilter does not benefit MVPA

Fig 3A shows the MVPA classification results as a function of time for the different pre-processing pipelines. We find that the use of the SSS filter significantly reduces the classification accuracy considering the 102 magnetometers, whereas the filter ("raw") and the SSP filter demonstrate similar results. Fig 3 B shows the comparison of the area under the curve value for "SSS" and "raw" conditions calculated from 150 ms to 450 ms after stimulus onset for each participant. This time interval is chosen to capture when the brain processes and encodes relevant information about the object category. It is evident from Fig. 3 that for 77% of the participants, classification is higher in the "raw" compared to the "SSS" condition. A paired t-test performed on the averaged classification accuracy (150 – 450 ms) to compare "raw" and "SSS" conditions yields a significant result ($t(30) = 3.448$, $p = 0.002$). "SSS" and "SSP" also show significant differences ($t(30) = 2.785$, $p=0.009$). A t-test performed on the mean classification accuracy for "raw" and "SSP" conditions is not significant ($t(30) = 0.856$, $p = 0.398$).

On the contrary, the application of the SSS filter does not lead to a significant decrease in MVPA classification when utilizing the 204 planar gradiometers (Fig. 4A) or all 306 sensors combined (Fig. 4B).

3.2. Magnetometers and Gradiometers

After optimizing the pre-processing pipeline, we compared the performance of 102 magnetometers and 102 gradiometers (no filter was applied). On each sensor location, one of two planar gradiometers was selected randomly. The results shown in Fig. 5 demonstrate similar performance for two types of sensors. No significant difference was found. The comparison of the AUC also showed no difference in accuracy between magnetometers and gradiometers. We conclude that when optimizing a MEG system for multivariate analysis, gradiometers and magnetometers work equally well.

3.3. Number of sensors

Finally, we investigated the impact of the number of sensors on MVPA classification accuracy. We assessed the classification performance using the area under the curve metric across 150 – 450 ms after a stimulus was presented. Fig 6 illustrates the relationship between AUC of classification as a function of a number of magnetometers (not using SSP or SSS condition). We observe that classification saturates at about 25 sensors.

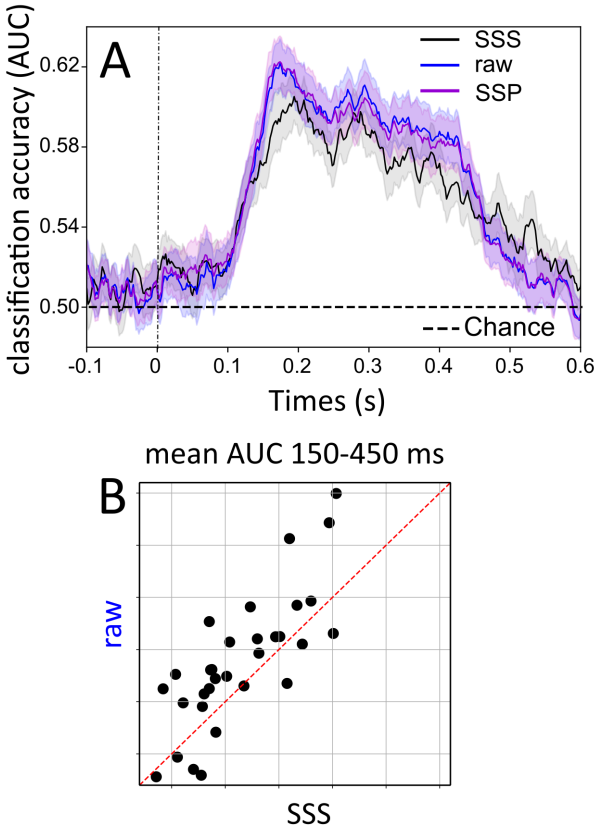

Figure 3: A) The time course of object categorization during image presentation for the unfiltered magnetometer ("raw") is shown in blue. The "SSS" filter is shown in black land "SSP" is shown in magenta. The highlighted area reflects the standard deviation error, while a dashed line signifies the chance level; B) Dots on the graph are the averaged AUC (150-450 ms) of the decoding curve for an individual subject. The comparison is made between the "raw" pipeline (y-axis) and the "SSS" pipeline (x-axis).

4. Discussion

We explored various noise reduction techniques for conventional MEG data in the context of MVPA analysis. The results demonstrate that the use of the SSP filter for denoising or no filter at all yields a significantly higher classification accuracy compared to when using the SSS filter. We also find there are no differences in classification accuracy when comparing a 102-magnetometer array to a 102-gradiometer array. Moreover, we show that

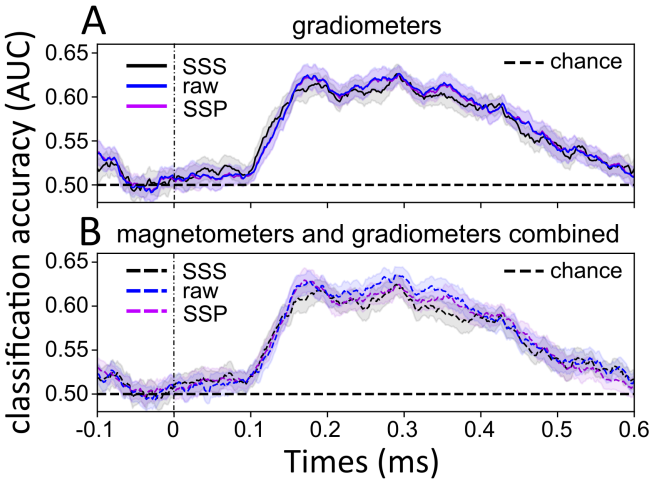

Figure 4: The time course of object categorization during image presentation for the unfiltered data ("raw") is shown in blue. The SSS filter is shown in magenta. A) The gradiometers data only. B) The magnetometer and gradiometer data combined. The highlighted area reflects the standard deviation error, while a dashed line signifies the chance level.

employing only 25 magnetometers evenly distributed over the head is sufficient to achieve classification accuracy comparable to a 102 magnetometer array.

Based on our results we do not recommend using SSS filter in OPM-MEG data when conducting MVPA. The implementation of SSS filters results in a significant reduction of the SVM classification accuracy when considering SQUID magnetometers. We attribute this decline in performance to the substantial rank reduction from 306 to 65 induced by the SSS filtering. This procedure may result in the exclusion of informative data important for classification based on MVPA. Since the classification curves with and without the SSP filter show no significant difference, we can conclude that noise artefacts do not impact classification accuracy in a "raw" condition.

Our results show that only magnetometers are significantly affected by the SSS filter, and we conclude that informative magnetometer data are attenuated by this method. No negative significant effect of SSS filtering was found when considering gradiometers or magnetometers and gradiometers combined (Fig. 4). In summary, to optimize noise reduction in MVPA for OPM-MEG system, we recommend considering methods such as SSP.

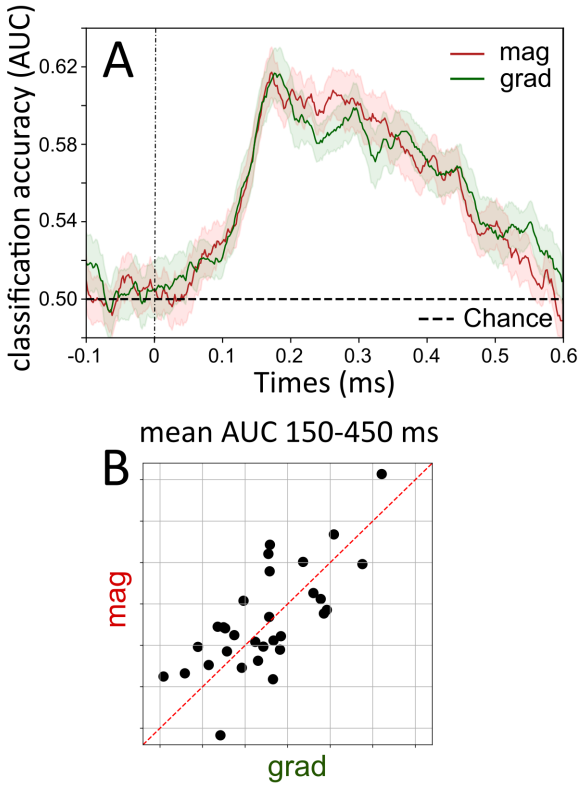

Figure 5: A) The time course of object categorization during image presentation for 102 gradiometers (green line) and for 102 magnetometers (red line). The highlighted area reflects the standard deviation error, while a dashed line signifies the chance level. B) Dots on the graph are the averaged AUC (150-450 ms) of the decoding curve for an individual subject. The comparison is made between classification results for magnetometers (y-axis) and gradiometers (x-axis). No difference was observed.

However other approaches such as ICA or 3rd-order gradient noise reduction might also be efficient (Vrba and Robinson, 2001). Note that 3rd-order gradient noise reduction requires a reference sensor array.

It is interesting that similar MVPA performance is observed between comparing arrays of magnetometers and gradiometers (Wens, 2023; Garcés et al., 2017). This could be explained by the fact that with 100 sensors, located 3 cm away from the brain, both gradiometers and magnetometers record sufficient information. As such, choosing between magnetometers and gradiometers does not seem to be a design consideration when optimizing an

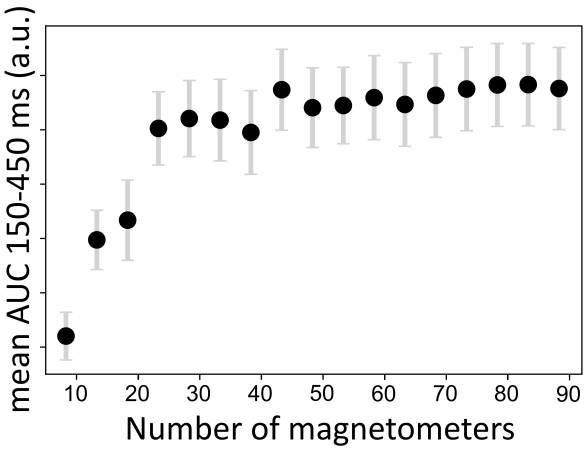

Figure 6: AUC of the decoding curve over time interval 150-450 ms after stimulus presentation is plotted as a function of the number of sensors in the magnetometer array.

MEG system for MVPA.

We showed that even with a relatively small number of magnetometers (25) in the array, the MVPA classification accuracy reaches saturation. It is surprising that a reduction from 102 to 25 sensors results in good classification accuracy considering that the rank reduction from 102 to 65 components by SSS reduced classification accuracy. Based on these findings, we suggest that when designing an OPM-MEG system for MVPA, 25 magnetometers may be sufficient.

In conclusion, MVPA has emerged as a powerful tool in cognitive neuroscience for detecting representational-specific neural patterns using M/EEG. Its application to OPM-MEG data holds great promise, particularly with the improved spatial coverage provided by the new system and the sensors being close to the head. Here we investigated the design considerations when utilizing OPM-MEG data for MVPA. We recommend recording data from at least 25 equally distributed OPMs. In terms of noise reduction, we do not recommend using SSS, but rather other approaches that do not reduce the rank of the data substantially such as SSP. Also, ICA or 3rd-order gradient noise reduction could be considered.

5. CRediT authorship contribution statement

Yulia Bezsudnova: Conceptualization; Formal analysis; Investigation; Methodology; Project administration; Visualization; Writing—Original draft; Writing—Review & editing. Ole Jensen: Conceptualization; Supervision; Funding Acquisition; Writing—Review & editing.

6. Declaration of Competing Interest

None.

7. Data availability

Raw data is available upon request and code can be accessed on https://github.com/Y-Bezs/cross-modal-project

8. Acknowledgments

The computations described in this paper were performed using the University of Birmingham's BEAR Cloud service, which provides flexible resources for intensive computational work to the University's research community. See http://www.birmingham.ac.uk/bear for more details. We thank Jonathan Winter for his support of MEG data acquisition. We also thank Andrew J. Quinn for help with statistical analysis, and Syanah Wynn for the fruitful discussions.

9. Funding information

This work was supported by the BBSRC (grant number BB/R018723/1), and an EPSRC (grant number EP/T001046/1). And a Wellcome Trust Investigator Award in Science (grant number 207550).

References

Ariani, G., Pruszynski, J.A., Diedrichsen, J., 2022. Motor planning brings human primary somatosensory cortex into action-specific preparatory states. elife 11, e69517.

Ashton, K., Zinszer, B.D., Cichy, R.M., Nelson III, C.A., Aslin, R.N., Bayet, L., 2022. Time-resolved multivariate pattern analysis of infant eeg data: A practical tutorial. Developmental cognitive neuroscience 54, 101094.

Beltrachini, L., von Ellenrieder, N., Eichardt, R., Haueisen, J., 2021. Optimal design of on-scalp electromagnetic sensor arrays for brain source localisation. Human brain mapping 42, 4869–4879.

Bezsudnova, Y., Koponen, L.M., Barontini, G., Jensen, O., Kowalczyk, A.U., 2022. Optimising the sensing volume of opm sensors for meg source reconstruction. NeuroImage 264, 119747.

Brainard, D.H., Vision, S., 1997. The psychophysics toolbox. Spatial vision 10, 433–436.

Brookes, M.J., Boto, E., Rea, M., Shah, V., Osborne, J., Holmes, N., Hill, R.M., Leggett, J., Rhodes, N., Bowtell, R., 2021. Theoretical advantages of a triaxial optically pumped magnetometer magnetoencephalography system. NeuroImage 236, 118025.

Brookes, M.J., Leggett, J., Rea, M., Hill, R.M., Holmes, N., Boto, E., Bowtell, R., 2022. Magnetoencephalography with optically pumped magnetometers (opm-meg): the next generation of functional neuroimaging. Trends in Neurosciences .

Brown, T.I., Carr, V.A., LaRocque, K.F., Favila, S.E., Gordon, A.M., Bowles, B., Bailenson, J.N., Wagner, A.D., 2016. Prospective representation of navigational goals in the human hippocampus. Science 352, 1323–1326.

Carlson, T.A., Grootswagers, T., Robinson, A.K., 2019. An introduction to time-resolved decoding analysis for m/eeg. arXiv preprint arXiv:1905.04820 .

Chan, A.M., Halgren, E., Marinkovic, K., Cash, S.S., 2011. Decoding word and category-specific spatiotemporal representations from meg and eeg. Neuroimage 54, 3028–3039.

Cheng, F., 2021. Using single-trial representational similarity analysis with eeg to track semantic similarity in emotional word processing. arXiv preprint arXiv:2110.03529 .

Cichy, R.M., Khosla, A., Pantazis, D., Torralba, A., Oliva, A., 2016. Comparison of deep neural networks to spatio-temporal cortical dynamics of human visual object recognition reveals hierarchical correspondence. Scientific reports 6, 27755.

Cichy, R.M., Pantazis, D., Oliva, A., 2014. Resolving human object recognition in space and time. Nature neuroscience 17, 455–462.

Cortes, C., Vapnik, V., 1995. Support-vector networks. Machine learning 20, 273–297.

Diedrichsen, J., Kriegeskorte, N., 2017. Representational models: A common framework for understanding encoding, pattern-component, and representational-similarity analysis. PLoS computational biology 13, e1005508.

Dirani, J., Pylkkänen, L., 2023. The time course of cross-modal representations of conceptual categories. NeuroImage 277, 120254.

Ferrante, O., Liu, L., Minarik, T., Gorska, U., Ghafari, T., Luo, H., Jensen, O., 2022. Flux: A pipeline for meg analysis. NeuroImage 253, 119047.

Frisby, S.L., Halai, A.D., Cox, C.R., Ralph, M.A.L., Rogers, T.T., 2023. Decoding semantic representations in mind and brain. Trends in cognitive sciences .

Garcés, P., López-Sanz, D., Maestú, F., Pereda, E., 2017. Choice of magnetometers and gradiometers after signal space separation. Sensors 17, 2926.

Gramfort, A., Luessi, M., Larson, E., Engemann, D.A., Strohmeier, D., Brodbeck, C., Goj, R., Jas, M., Brooks, T., Parkkonen, L., et al., 2013. Meg and eeg data analysis with mne-python. Frontiers in neuroscience , 267.

Grootswagers, T., Wardle, S.G., Carlson, T.A., 2017. Decoding dynamic brain patterns from evoked responses: a tutorial on multivariate pattern analysis applied to time series neuroimaging data. Journal of cognitive neuroscience 29, 677–697.

Guggenmos, M., Sterzer, P., Cichy, R.M., 2018. Multivariate pattern analysis for meg: A comparison of dissimilarity measures. Neuroimage 173, 434–447.

Harrison, S.A., Tong, F., 2009. Decoding reveals the contents of visual working memory in early visual areas. Nature 458, 632–635.

Haumann, N.T., Parkkonen, L., Kliuchko, M., Vuust, P., Brattico, E., et al., 2016. Comparing the performance of popular meg/eeg artifact correction methods in an evoked-response study. Computational intelligence and neuroscience 2016.

Haxby, J.V., Gobbini, M.I., Furey, M.L., Ishai, A., Schouten, J.L., Pietrini, P., 2001. Distributed and overlapping representations of faces and objects in ventral temporal cortex. Science 293, 2425–2430.

Haynes, J.D., Rees, G., 2006. Decoding mental states from brain activity in humans. Nature reviews neuroscience 7, 523–534.

Huth, A.G., Nishimoto, S., Vu, A.T., Gallant, J.L., 2012. A continuous semantic space describes the representation of thousands of object and action categories across the human brain. Neuron 76, 1210–1224.

Hyvärinen, A., Oja, E., 2000. Independent component analysis: algorithms and applications. Neural networks 13, 411–430.

Iamshchinina, P., Karapetian, A., Kaiser, D., Cichy, R.M., 2022. Resolving the time course of visual and auditory object categorization. Journal of Neurophysiology 127, 1622–1628.

Iivanainen, J., Stenroos, M., Parkkonen, L., 2017. Measuring meg closer to the brain: Performance of on-scalp sensor arrays. NeuroImage 147, 542–553.

Kaplan, J.T., Man, K., Greening, S.G., 2015. Multivariate cross-classification: applying machine learning techniques to characterize abstraction in neural representations. Frontiers in human neuroscience 9, 151.

King, J.R., Dehaene, S., 2014. Characterizing the dynamics of mental representations: the temporal generalization method. Trends in cognitive sciences 18, 203–210.

Konkle, T., Caramazza, A., 2013. Tripartite organization of the ventral stream by animacy and object size. Journal of Neuroscience 33, 10235–10242.

Kornysheva, K., Bush, D., Meyer, S.S., Sadnicka, A., Barnes, G., Burgess, N., 2019. Neural competitive queuing of ordinal structure underlies skilled sequential action. Neuron 101, 1166–1180.

Kriegeskorte, N., 2009. Relating population-code representations between man, monkey, and computational models. Frontiers in Neuroscience 3, 879.

Kriegeskorte, N., Kievit, R.A., 2013. Representational geometry: integrating cognition, computation, and the brain. Trends in cognitive sciences 17, 401–412.

Kriegeskorte, N., Mur, M., Bandettini, P.A., 2008. Representational similarity analysis-connecting the branches of systems neuroscience. Frontiers in systems neuroscience , 4.

Labyt, E., Sander, T., Wakai, R., 2022. Flexible High Performance Magnetic Field Sensors: On-Scalp Magnetoencephalography and Other Applications. Springer Nature.

Nugent, A.C., Andonegui, A.B., Holroyd, T., Robinson, S.E., 2022. On-scalp magnetocorticography with optically pumped magnetometers: Simulated performance in resolving simultaneous sources. Neuroimage: Reports 2, 100093.

Pedregosa, F., Varoquaux, G., Gramfort, A., Michel, V., Thirion, B., Grisel, O., Blondel, M., Prettenhofer, P., Weiss, R., Dubourg, V., et al., 2011. Scikit-learn: Machine learning in python. Journal of machine learning research 12, 2825–2830.

Pereira, F., Mitchell, T., Botvinick, M., 2009. Machine learning classifiers and fmri: a tutorial overview. Neuroimage 45, S199–S209.

Proklova, D., Kaiser, D., Peelen, M.V., 2016. Disentangling representations of object shape and object category in human visual cortex: The animate–inanimate distinction. Journal of cognitive neuroscience 28, 680–692.

Rea, M., Boto, E., Holmes, N., Hill, R., Osborne, J., Rhodes, N., Leggett, J., Rier, L., Bowtell, R., Shah, V., et al., 2022. A 90-channel triaxial magnetoencephalography system using optically pumped magnetometers. Annals of the New York Academy of Sciences 1517, 107–124.

Stokes, M.G., Wolff, M.J., Spaak, E., 2015. Decoding rich spatial information with high temporal resolution. Trends in cognitive sciences 19, 636–638.

Taulu, S., Kajola, M., 2005. Presentation of electromagnetic multichannel data: the signal space separation method. Journal of Applied Physics 97.

Taulu, S., Simola, J., 2006. Spatiotemporal signal space separation method for rejecting nearby interference in meg measurements. Physics in Medicine & Biology 51, 1759.

Tyler, L.K., Cheung, T.P., Devereux, B.J., Clarke, A., 2013. Syntactic computations in the language network: characterizing dynamic network properties using representational similarity analysis. Frontiers in psychology 4, 271.

Uusitalo, M.A., Ilmoniemi, R.J., 1997. Signal-space projection method for separating meg or eeg into components. Medical and biological engineering and computing 35, 135–140.

Vrba, J., Robinson, S., 2001. The effect of environmental noise on magnetometer-and gradiometer-based meg systems. Signal 1, 0–5.

Wang, L., Kuperberg, G., Jensen, O., 2018. Specific lexico-semantic predictions are associated with unique spatial and temporal patterns of neural activity. Elife 7, e39061.

Wens, V., 2023. Exploring the limits of meg spatial resolution with multipolar expansions. NeuroImage 270, 119953.